Current Applied Physics 10 (2010) 1046–1052

Contents lists available at ScienceDirect

Current Applied Physics

journal homepage: www.elsevier.com/locate/cap

Aspect ratio control of acid modified multiwalled carbon nanotubes

Don-Young Kim, Young Soo Yun, Hyeonseong Bak, Se Youn Cho, Hyoung-Joon Jin *

Department of Polymer Science and Engineering, Inha University, Incheon 402-751, Republic of Korea

ARTICLE INFO

Article history:
Received 31 July 2009
Received in revised form 7 November 2009
Accepted 22 December 2009
Available online 28 December 2009

Keywords:
Carbon nanotubes
Aspect ratio
Electrical conductivity
Polymer composites

ABSTRACT

This study examined the effects of acid treatments on the length of multiwalled carbon nanotubes (MWCNTs) as well as the influence of the aspect ratio of the MWCNTs on the electrical percolation threshold. In particular, the length distribution, intensity ratio of the G and D Raman peaks, BET surface area, and maximum decomposition temperatures of the MWCNTs were investigated. The MWCNTs showed different electrical percolation thresholds depending on the aspect ratio. The higher aspect ratio MWCNTs had lower electrical percolation thresholds than those with smaller ratios due to their ease of contact with other MWCNTs. In terms of the electrical behavior of a MWCNT film, many more short MWCNTs were necessary to reach the electrical percolation threshold than long MWCNTs. These results demonstrate the need to control the aspect ratio of MWCNTs in order for them to be used efficiently in electrical applications.

1. Introduction

Since the landmark paper by Iijima in 1991, carbon nanotubes (CNTs) have attracted considerable attention on account of their excellent mechanical, electrical and thermal properties [1]. Therefore, they offer many opportunities for the development of novel material systems [2–4]. Many methods for synthesizing CNTs have been reported. Currently, CNT growth processes, such as chemical vapor deposition (CVD), are based on the use of transition metal catalysts [5,6]. CNT synthesis by CVD is a promising route for the bulk production of high purity CNTs suitable for commercialization. However, pristine CNTs contain other carbonaceous impurities, such as amorphous carbon, nanocrystalline graphite and metallic catalysts. These impurities limit the performance of CNTs and hinder their potential applications to new material systems. A common route for eliminating these impurities is liquid phase chemical oxidation by acid treatments. This route induces the formation of various functional groups, such as carboxyl groups, which can increase the dispersibility of CNTs [7–10]. This method also causes CNT cutting. Many methods reported for cutting CNTs begin with chemical oxidation [9–14]. It is expected that CNTs with various lengths can be used in a variety of fields, such as electronic, biological, and composite materials [9,13,15]. Recently, ball milling has been reported to be an efficient method for cutting CNTs [16,17]. However, it normally takes a long time to produce sufficiently short CNTs. Moreover, this method requires a purification process. Therefore, CNT cutting with acid treatments is more suitable than ball milling because it also includes a purification and functionalization process. CNT length reduction by an acid treatment depends heavily on the oxidation time, which means that the aspect ratio of CNTs can be controlled by the oxidation time [9–11].

CNTs have attracted considerable interest as conducting fillers owing to their superior electric conductivity. Thin CNT films or polymer/CNT composites usually exhibit a lower percolation threshold than materials loaded with other fillers because of their high intrinsic conductivity and high aspect ratio [18]. An increase in the aspect ratio of CNT increases their Young's modulus and reduces the critical concentration of percolation network seeds [19]. The preparation of well-dispersed multiwalled carbon nanotubes (MWCNTs) becomes difficult with increasing CNT aspect ratio [20,21]. High aspect ratio CNTs agglomerate easily, which often reduces their physical properties, particularly the electrical percolation threshold in thin CNT films or CNT/polymer composites [22]. In addition, CNTs are typically synthesized to polydisperse micrometer lengths and fiber like shapes. Recently, the potential toxicity of CNTs has attracted attention because of their apparent similarity to asbestos and other carcinogenic fibers. In particular, it has been reported that the toxicity of short tangled CNTs is lower than that of long straight ones [23]. Reducing the potential toxicity of bio-related materials is clearly of high importance. For these reasons, control of the CNT aspect ratio is essential if they are to be used in many applications. This study examined the effects of acid treatments on the length of MWCNTs as well as the influence of the aspect ratio of MWCNT on the electrical percolation threshold.

* Corresponding author. Tel.: +82 32 860 7483; fax: +82 32 865 5178.
E-mail address: hjjin@inha.ac.kr (H.-J. Jin).

1567-1739/$ - see front matter © 2009 Elsevier B.V. All rights reserved.
doi:10.1016/j.cap.2009.12.038

2. Experimental

2.1. Materials

MWCNTs (95% pure, supplied by Iljin Nanotech, Korea) were produced by CVD. Sulfuric acid (H_2SO_4, 98%, DC Chemical Co. Ltd., Korea) and nitric acid (HNO_3, 70%, DC Chemical Co. Ltd., Korea) were purchased and used as received. Cetyl trimethylammonium bromide (CTAB, Aldrich, USA) and polyvinylpyrrolydone (PVP, M_w: 360,000 g/mol, Aldrich, USA) were used without further purification.

2.2. Preparation of aspect ratio controlled MWCNTs

Pristine MWCNTs were suspended in HCl and stirred for 2 h with a magnetic stirrer. The resulting purified MWCNTs were renamed "MWCNT 7" due to their average length of 7 μm. The MWCNT 7 were suspended in a mixture of condensed H_2SO_4 and HNO_3 (3:1 volume ratios) and heated under refluxed at 60 °C for 3 or 24 h. The resulting acid-treated MWCNTs were renamed "MWCNT 3" and "MWCNT 1" due to their average lengths of 3 and 1 μm, respectively. The MWCNTs were washed several times with deionized water until the pH of the rinsing water was neutral, and then dried in a vacuum oven at 25 °C for 2 days.

2.3. High-temperature annealing of the acid-treated MWCNTs

The acid-treated MWCNTs were placed in the center of a horizontal electric resistance tube furnace (High Temp. Furnace, Ajeon Heating Industrial Co., Ltd., Korea) and heated to 1600 °C at a rate of 10 °C/min. The samples were held at this temperature for 3 h at pressures <10 Pa to prevent oxidation. The lowest pressure was 10^{-3} Pa.

2.4. Preparation of MWCNT film

CTAB was used to prepare an aqueous MWCNT dispersion of the MWCNT samples. The concentration of the surfactant was approximately 0.3 wt.%, and the MWCNT concentration used for the homogeneous dispersion was 0.01 wt.%. The aqueous MWCNT dispersions were diluted one hundred times. The final diluted MWCNT aqueous solutions (1.0×10^{-4} wt.%) were filtered through a 0.2 mm mesh ceramic filter. The CTAB surfactant was rinsed with deionized water before drying under a vacuum at 25 °C.

2.5. Preparation of PVP/MWCNT composites

A 100 ml flask containing a predetermined amount of MWCNTs, 3.0 g of PVP and deionized water was sonicated at 600 W for 20 min (Kodo Technical Research, Korea). The mixture was then dried in a vacuum oven at 25 °C for 2 days.

2.6. Characterization

The morphology and average length of the MWCNTs was observed by preparing the samples using a ceramic filter (pore size; 0.2 μm, diameter; 47 mm, Whatman, UK). The MWCNTs captured by the ceramic filter were examined by scanning electron microscopy (SEM, Hitachi, S-4300, Japan). Transmission electron microscopy (TEM, Philips, CM200, 200 kV accelerating voltage, USA) was used to observe the morphology of the MWCNTs on copper grids. The thermal stability and mass loss of the MWCNTs was estimated by thermogravimetric analysis (TGA, TA instruments, Q50, UK) at a heating rate of 20 °C/min ranging from room temperature to 800 °C in air. Raman spectroscopy (BRUKER RFS-100/S, 1064 nm

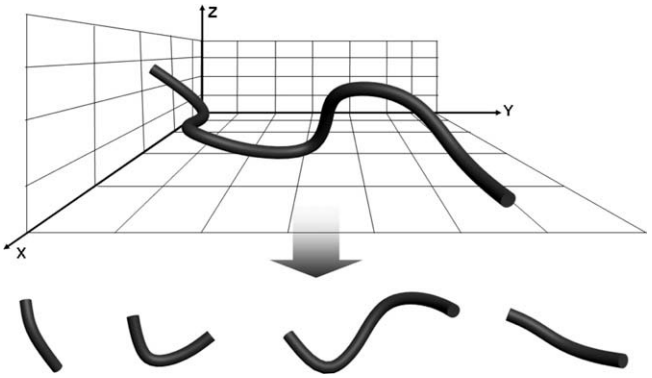

Fig. 1. Schematic diagram of the cutting process of MWCNTs by acid treatment.

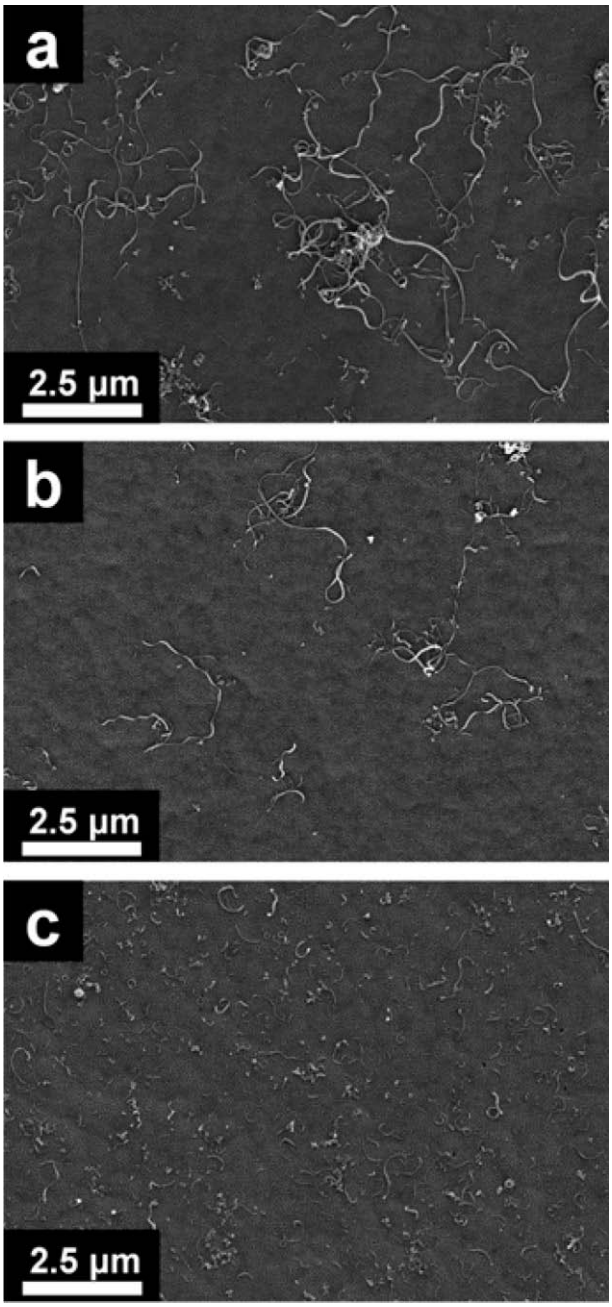

Fig. 2. SEM image of (a) MWCNT 7, (b) MWCNT 3, and (c) MWCNT 1 films.

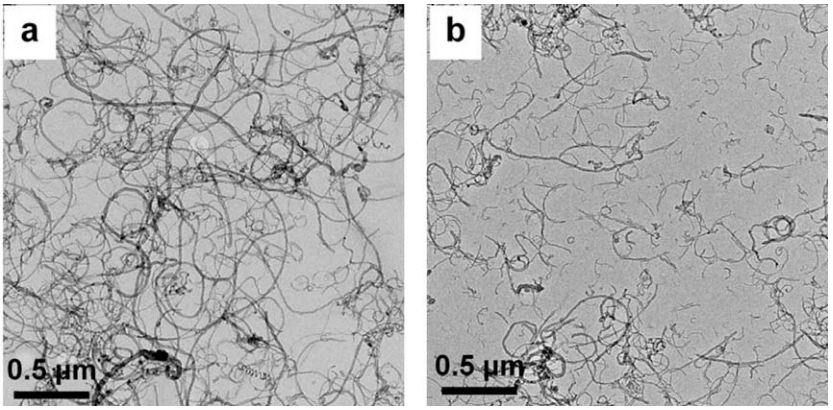

Fig. 3. TEM image of (a) MWCNT 3 and (b) MWCNT 1.

Table 1
Characteristics of the acid-treated and high-temperature annealed MWCNTs.

	MWCNT 7	MWCNT 3	MWCNT 1
Average length (μm)	7.0 ± 2	3.0 ± 0.8	0.9 ± 0.5
Average diameter (nm)	13 ± 3	13 ± 3	8 ± 2
S_{BET} (m^2/g)	116	183	391
I_G/I_D ratio			
Before annealing	0.85	0.76	0.72
After annealing	1.06	0.81	0.80
MDT (°C)			
Before annealing	649	622	613
After annealing	682	633	632
Metal catalyst residues (%)			
Before annealing	2.6	1.7	1.5
After annealing	5.3	3.2	1.5

excitation, Germany) was used to determine the presence of sp^2 hybridized carbon by examining the E_{2g} mode or G band (stretching vibrations in the basal plane of crystalline graphite), the so-called D band (indicating the level of defects in the graphitic material), and the I_G/I_D ratio (D band to G band intensity ratio, which is normally used to assess the purity and crystallinity) of the MWCNT samples. The MWCNT surface areas were determined from the nitrogen adsorption–desorption isotherms using a porosimetry analyser (Micromeritics, ASAP 2020, USA) at 77 K. The Brunauer–Emmett–Teller (BET) surface areas (S_{BET}) were calculated using BET theory. The UV–vis optical absorbance spectra of the MWCNT dispersions were obtained using an Agilent 8453 UV–visible spectrophotometer (Agilent Technologies, Germany). The stability of the MWCNT dispersions was monitored by measuring the transmittance and back-scattering of pulsed near infrared light (λ = 880 nm). The transmittance detector received light that passed directly through the dispersion (at an angle of 180° with respect to the source), while the back-scatter detector received light (back) scattered by 45°. The detection head scanned the entire height of the sample acquiring the transmittance and back-scattering data in 40 μm steps every 24 h for 72 h. The sheet resistance of the MWCNT films and volume resistivity of the PVP/MWCNT composites were measured using a four-probe equipped with a resistivity meter (Mitsubishi Chemical Hiresta-up MCP-HT 450, Japan).

3. Results and discussion

The as-produced MWCNTs contained carbonaceous impurities, such as amorphous carbon, nanocrystalline graphite, and metallic catalysts. Therefore, considerable effort has been made to purifying them, such as the use of acid treatments. In addition, the pentagonal, heptagonal, and vacancy defects in the MWCNTs tended to bend and twist their structure [24,25]. Oxidative damage can be induced at these defect sites. The sp^3 carbon atoms of defects in the MWCNTs are first attacked by oxidation, which ultimately etches the MWCNTs [26]. Therefore, an acid treatment can be used to control the aspect ratio of the MWCNTs (Fig. 1). Many studies also examined CNT cutting using this phenomena. Acid treatments are more advantageous than other methods because of the ability to integrate the purification, cutting, and functionalization steps. For this reason, a 3:1 H_2SO_4:HNO_3 solution was prepared to control the MWCNT aspect ratios by varying the oxidation time [9,13,14].

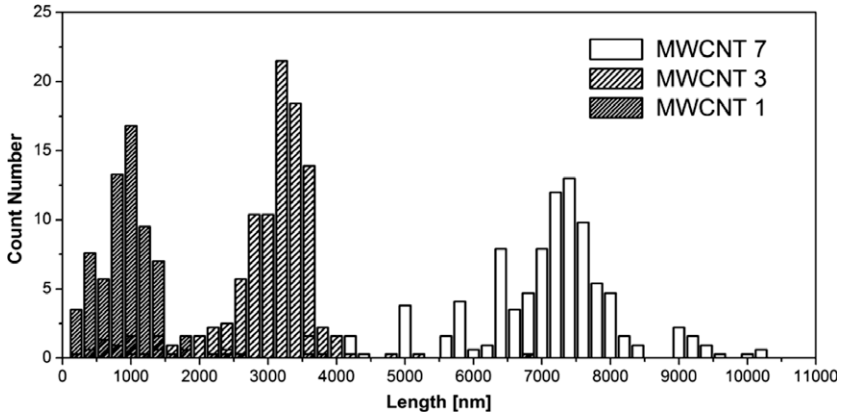

Fig. 4. The length distribution of the aspect ratio controlled MWCNT samples.

The aspect ratios of the MWCNTs differed according to the acid treatment time (Figs. 1–3). SEM and TEM analyses indicated a decrease in the average length and diameter of the MWCNTs with increasing oxidation time. Table 1 lists the corresponding average length and diameter. Fig. 4 shows the length distribution of the aspect ratio controlled MWCNT samples. The change in length of the MWCNTs with the oxidation time corresponded to expectations.

Raman spectroscopy, TGA, and BET were used to confirm the change in MWCNT structure. The G-band: D-band intensity ratio (I_G/I_D) in the Raman spectra is often used to evaluate defects in CNTs. The I_G/I_D ratio of MWCNT 7, MWCNT 3, and MWCNT 1 was 0.85, 0.76, and 0.72, respectively (Fig. 5). This indicates that the marked decrease observed after the acid treatment was due to the increase in defects. One of the most common defects in MWCNTs is an open end caused by cutting, which can have a significant effect on the I_G/I_D ratio.

TGA and BET analyses also demonstrated a change in the structure of the MWCNTs. Fig. 6 shows various MWCNT samples with different maximum decomposition temperatures (MDT). According to acid-treated time, MWCNTs have a large amount of defect. The defects of MWCNTs attenuate their thermal resistance. Therefore, MWCNT 7 had relatively high maximum decomposition temperatures (MDT) compared with MWCNT 3 and MWCNT 1 (Fig. 6a and b). This result corresponds to the Raman data. The defects of MWCNTs were reduced by high-temperature annealing. Therefore, The MDTs of the high-temperature annealed MWCNTs were higher than that of the acid-treated MWCNTs (Fig. 6c and d). The BET surface area (S_{BET}) of the acid-treated MWCNTs was higher than that of the pristine MWCNTs. The increasing S_{BET} of the MWCNT samples was attributed to a decrease in the MWCNT length, open-endedness, and the removal of metallic catalysts and amorphous carbon during the acid treatment. The latter leads to structural alterations, particularly the length of the MWCNTs, which can allow control of the MWCNT aspect ratios. Finally, the length of the MWCNTs depends on the oxidation time. Overall, the MWCNT length was reduced by the acid treatment, and the MWCNT aspect ratio was controlled by the oxidation time.

The influence of the MWCNT aspect ratio on the electrical percolation threshold was examined. However, the acid treatment induced structural changes to the MWCNTs, which created defects that had significant effects on the thermal, mechanical, and electrical properties. This follows from the strong dependence of MWCNT properties on the graphitic structure. Since the structure of CNTs is similar to that of graphite, it is reasonable

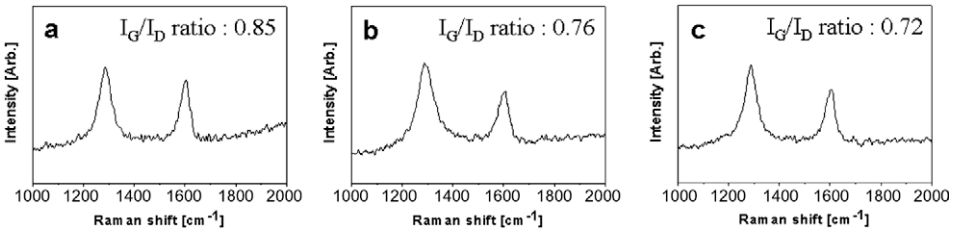

Fig. 5. Raman spectra of the MWNTs according to the acid treatment time. (a) MWNT 7, (b) MWNT 3, and (c) MWNT 1.

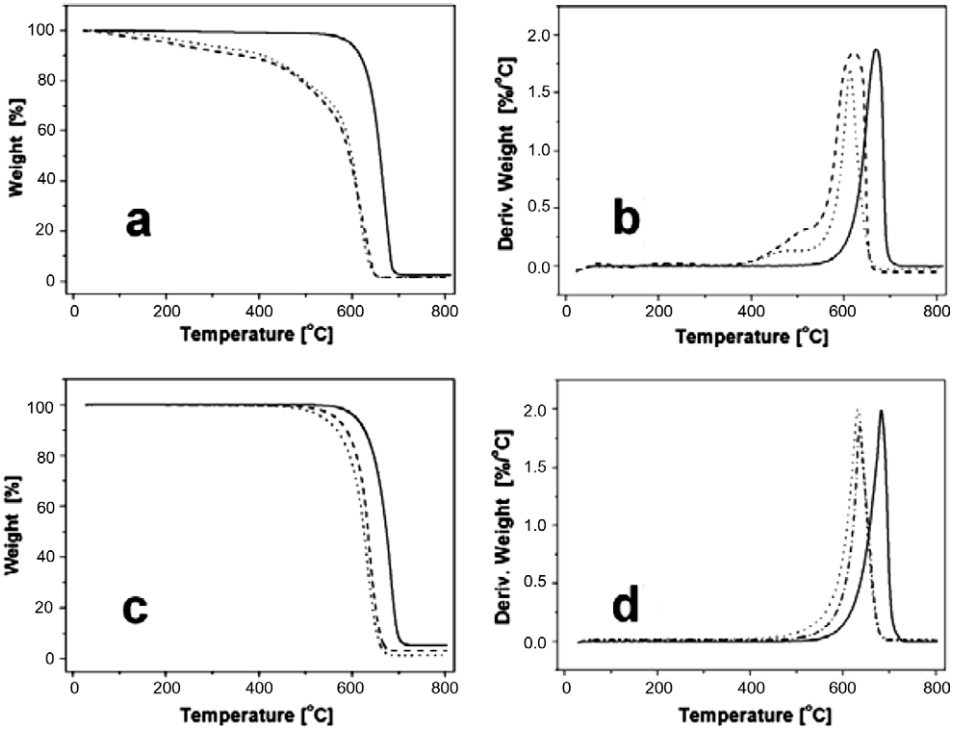

Fig. 6. TGA and DTA curves in air of the (a, b) acid-treated MWCNTs and (c, d) high-temperature annealed MWCNTs. The solid line is MWCNT 7, the dashed line is MWCNT 3, and the dotted line is MWCNT 1.

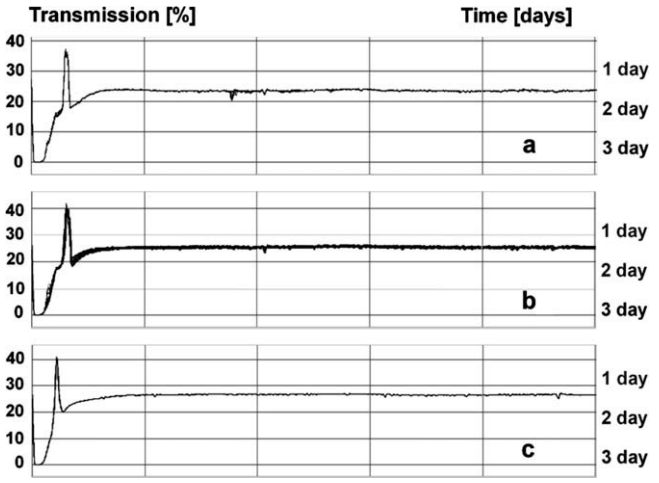

Fig. 7. Turbiscan data of the aqueous MWCNT dispersions ((a) MWCNT 7, (b) MWCNT 3 and (c) MWCNT 1).

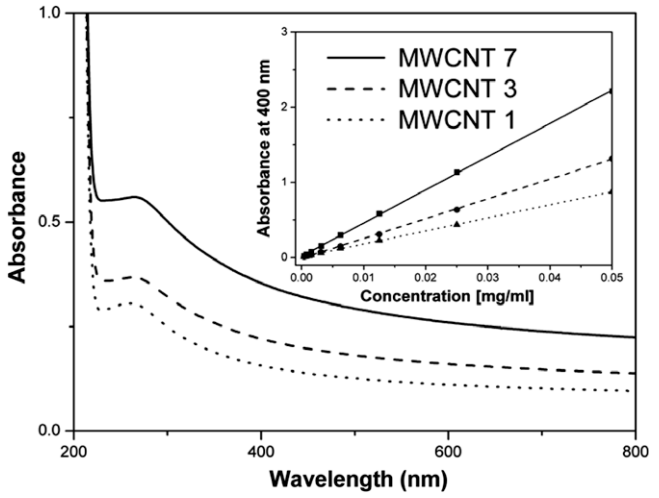

Fig. 8. UV–vis spectra of the aqueous MWCNT dispersion (0.001 wt.%). Inset: absorbance at 400 nm of the aspect ratio controlled MWCNTs as a function of the concentration.

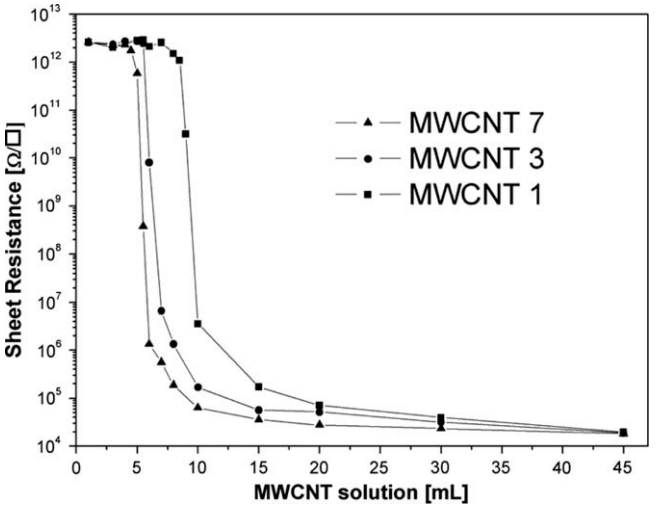

Fig. 9. Sheet resistance of the MWCNT films with aspect ratio controlled MWCNTs.

to assume that a theoretical model developed for graphite would also be applicable. For this reason, many researchers have examined the healing of defects in CNTs using high-temperature annealing [27,28].

High-temperature annealing is used to remove these defects. The I_G/I_D ratio of the high-temperature annealed MWCNTs increased compared to the non-annealed samples without considerable changes to their average length and diameter (Table 1). Fig. 6 and Table 1 show the effects of the acid treatment and high-temperature annealing on the oxidative stability of the MWCNT samples [29,30]. The MDT of the high-temperature annealed MWCNTs was higher than that of the acid-treated MWCNTs. At low pressure, high-temperature annealing is used to remove these defects because of a reduction reaction. As the sp^3 carbon atoms on mainframe of MWCNT changed to the sp^2 carbon atoms, the I_G/I_D

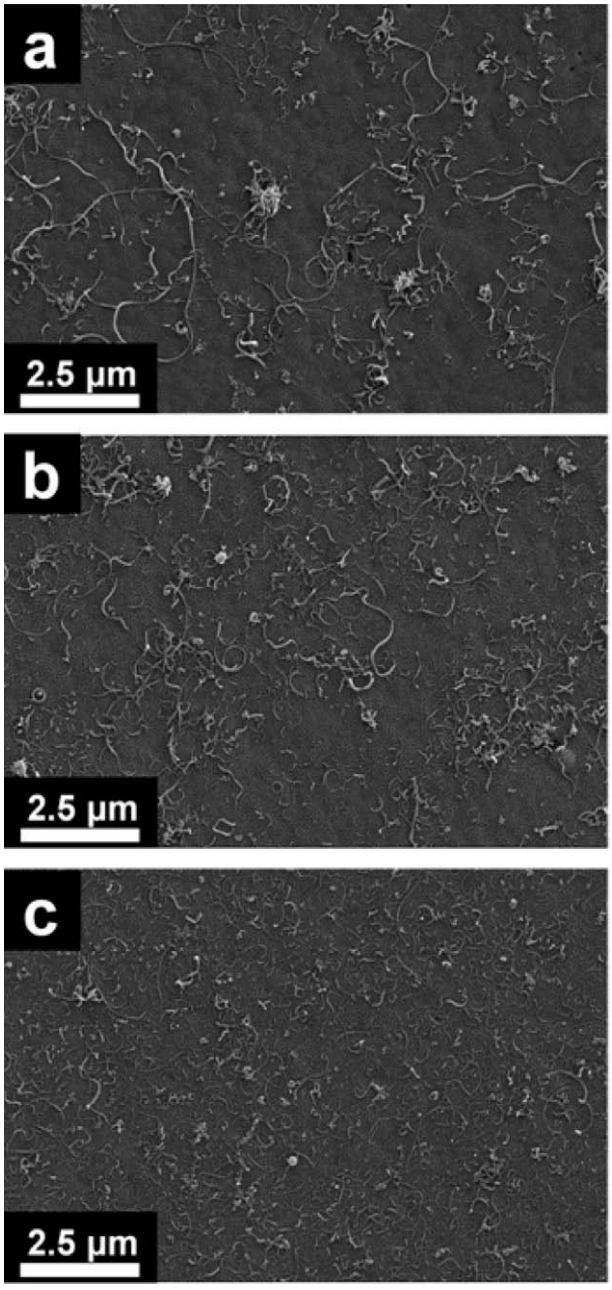

Fig. 10. SEM image of the MWCNT films at the electrical percolation threshold ((a) MWCNT 7 (4.5 ml), (b) MWCNT 3 (5.5 ml), and (c) MWCNT 1 (8.5 ml)).

ratios of MWCNTs were increased and thermal stability of MWCNTs was higher than that of the acid-treated MWCNTs. In addition, in accordance with removing amorphous carbon and other carbon fragments, the relative weights of metal catalyst residue are increased.

The effect of length on the electrical conductivity of the MWCNTs was examined. Networks and arrays of CNTs as films on a substrate (2D) and CNT/polymer composites (3D) have attracted considerable attention due to their potential applications, particularly as conducting materials. The attractive feature of these materials is that the CNT aspect ratio can affect the electrical percolation behavior. Therefore, the 2D and 3D percolation behavior with the aspect ratio controlled MWCNTs was investigated. Uniform films of MWCNTs were produced by vacuum filtering a dilute dispersion of MWCNT samples in water over a ceramic with a pore size of 0.2 μm. The production of uniform MWCNT films using a dilute dispersion of MWCNTs requires them to be homogeneous and stable. Therefore, the stability of the MWCNT dispersion was characterized using a Turbiscan [10,31]. Fig. 7 presents the transmittance profiles obtained from the MWCNT dispersions of 0.005 wt.% MWCNTs and 0.3 wt.% surfactant. The resulting profile was plotted as the transmittance intensity of the light passed through the dispersions versus the height of the dispersion within a test cell. All the profiles of MWCNT dispersion were constant over 3 days. This means that the MWCNT dispersion is stable and not aggregated or precipitated. The profiles of MWCNT dispersion would surge irregularly if the MWCNTs are aggregated or precipitated. MWCNT dispersion stability was also characterized by UV–vis spectroscopy. Fig. 8 (inset) shows the change in absorbance at 400 nm as a function of the MWCNT sample concentration. The optical absorbance at 400 nm increased linearly with increasing MWCNT concentration according to the Lambert–Beer law [32]. This shows the aqueous MWCNT dispersion is in a homogeneous dispersion state. Two aspects of the aqueous MWCNT dispersion can be found using UV–vis spectra. First, the strong peak at approximately 265 nm shows that the MWCNTs 7, 3 and 1 samples show characteristic peak of carbon nanotubes. Second, regardless of the MWCNT concentration and wavelength, the absorption data shows a clear dependence on the average length of the MWCNTs (Fig. 8).

This was attributed to the fact that the volume occupied by a single nanotube depends approximately on R^3, where R is the overall size of the nanotube. $R = 2l_{sp} \times L$ in the random coil limit, where l_{sp} is the persistence length of the CNT, and L is the contour length of the CNT [33]. The fully occupied concentration may depend on L when nanotubes are dispersed in an overall body centered cubic (bcc) structure. Therefore, light transmittance increases with decreasing nanotube length when their static bending persistence lengths are the same. In particular, the optical absorbance increases with increasing average MWCNT length, and the electrical percolation threshold depends on the length of the MWCNT.

Fig. 9 shows the 2D percolation behavior, which explains the effects of the aspect ratio of the MWCNT on the sheet electrical resistivity of the MWCNT film. Increasing the nanotube aspect ratio leads to a low percolation threshold. Fig. 10 shows SEM images of the MWCNT 7, MWCNT 3, and MWCNT 1 prepared by filtering a volume of 4.5, 5.5 and 8 ml (The aqueous MWCNT dispersion is 1.0×10^{-4} wt.%), respectively, at the electrical percolation threshold point. For 2D percolation, many more MWCNT 1 were required to reach the electrical percolation threshold than MWCNT 7. For

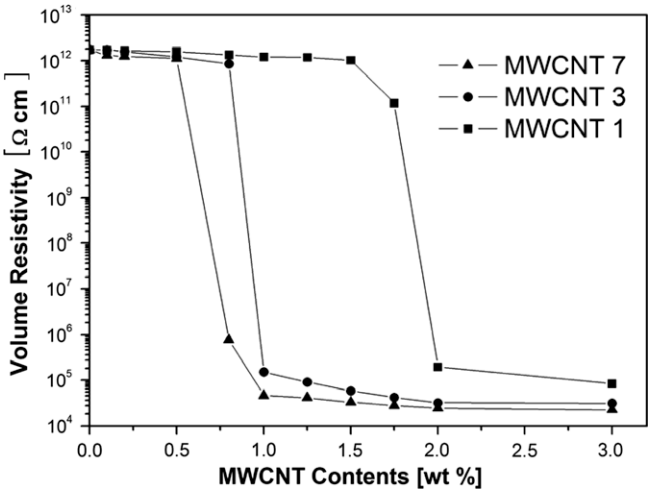

Fig. 11. Sheet resistance of the PVP/MWCNT composites with the aspect ratio controlled MWCNTs.

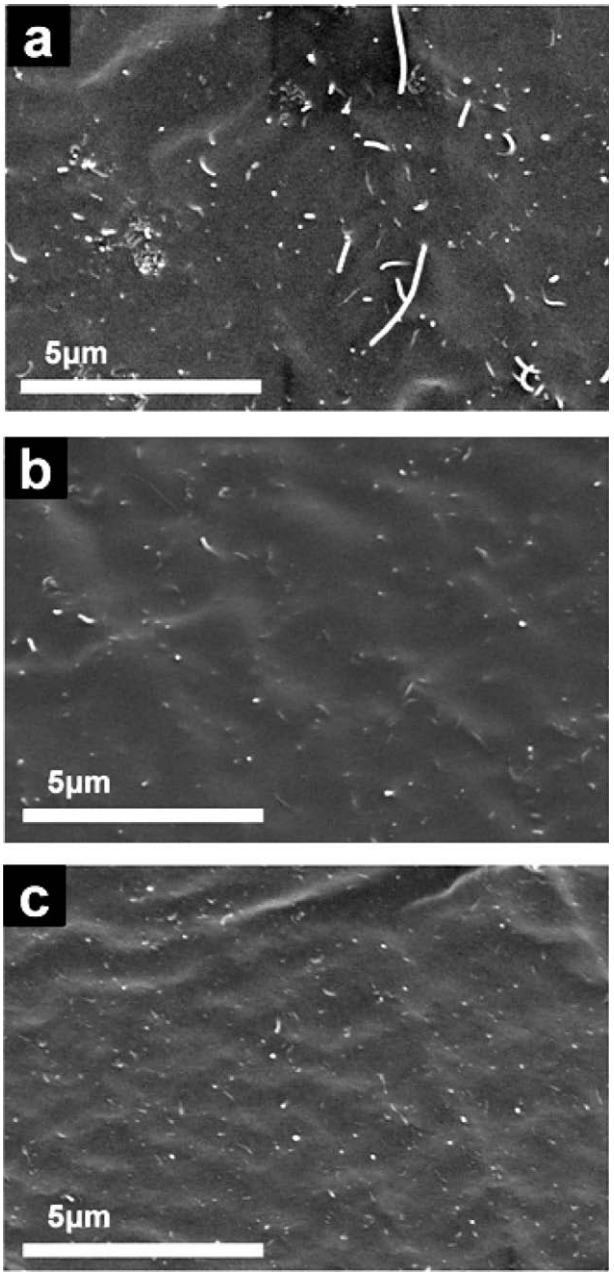

Fig. 12. SEM image of the fracture surface of PVP/MWCNT (1.0 wt.%) composites ((a) MWCNT 7, (b) MWCNT 3, and (c) MWCNT 1).

the 3D percolation behavior, polymer/MWCNT composites were prepared to examine the effect of the aspect ratio (Fig. 11).

The higher aspect ratio MWCNTs showed a lower electrical percolation threshold. Fig. 12 displays the fracture surface of the PVP/MWCNT composites. As previously shown, the dispersion state of the MWCNTs has a significant effect on the MWCNT percolation threshold. The fracture surface showed that all types of MWCNTs were well-dispersed in the polymer matrix. The electrical percolation threshold decreased with increasing MWCNT aspect ratio (Figs. 9 and 11).

4. Conclusions

Aspect ratio controlled MWCNTs were prepared by varying the acid treatment time. The length distribution, I_G/I_D ratio, S_{BET}, and MDT of the MWCNTs were examined. The aspect ratio controlled MWCNTs showed different electrical percolation thresholds. The higher aspect ratio MWCNTs had lower electrical percolation thresholds because of their ease of contact with other MWCNTs. These results demonstrate that the aspect ratio of MWCNTs must be controlled in order for them to be used efficiently in electrical applications.

Acknowledgements

This work was supported by a Korea Science and Engineering Foundation (KOSEF) grant funded by the Korean Government (MEST) (R11-2005-065) through the Intelligent Textile System Research Center (ITRC).

References

[1] S. Iijima, Nature 354 (1991) 56–58.
[2] J.H. Sung, H.S. Kim, H.-J. Jin, H.J. Choi, J.J. Chin, Macromolecules 37 (2004) 9899–9902.
[3] P.M. Ajayan, L.S. Schadler, C. Giannaris, A. Rubio, Adv. Mater. 12 (2000) 750–753.
[4] H.-J. Jin, H.J. Choi, S.H. Yoon, S.J. Myung, S.E. Shim, Chem. Mater. 17 (2005) 4034–4037.
[5] R. Andrews, D. Jacques, D. Qian, T. Rantell, Acc. Chem. Res. 35 (2002) 1008–1017.
[6] G.S.B. McKee, K.S. Vecchio, J. Phys. Chem. B 110 (2006) 1179–1186.
[7] H.S. Kim, M. Kang, W.I. Park, D.Y. Kim, H.-J. Jin, Mod. Phys. Lett. B 22 (2008) 2493–2501.
[8] J. Zhang, H. Zou, Q. Qing, Y. Yang, Q. Li, Z. Liu, X. Guo, Z. Du, J. Phys. Chem. B 107 (2003) 3712–3718.
[9] J. Liu, A.G. Rinzler, H. Dai, J.H. Hafner, R.K. Bradley, P.J. Boul, A. Lu, T. Iverson, K. Shelimov, C.B. Huffman, F.R. Macias, Y.-S. Shon, T.R. Lee, D.T. Colbert, R.E. Smally, Science 280 (1998) 1253–1256.
[10] G.A. Forrest, A.J. Alexander, J. Phys. Chem. C 111 (2007) 10792–10798.
[11] K.J. Ziegler, Z. Gu, H. Peng, E.L. Flor, R.H. Hauge, R.E. Smalley, J. Am. Chem. Soc. 127 (2005) 1541–1547.
[12] K.J. Ziegler, Z. Gu, J. Shaver, Z. Chen, E.L. Flor, D.J. Schmidt, C. Chan, R.H. Hauge, R.E. Smalley, Nanotechnology 16 (2005) S539–S544.
[13] X.X. Wang, J.N. Wang, H. Chang, Y.F. Zhang, Adv. Funct. Mater. 17 (2007) 3613–3618.
[14] Y. Liu, L. Gao, J. Sun, S. Zheng, L. Jiang, Y. Wang, H. Kajiura, Y. Li, K. Noda, Carbon 45 (2007) 1972–1978.
[15] X.X. Wang, J.N. Wang, Carbon 46 (2008) 117–125.
[16] A. Kukovecz, T. Kanyó, Z. Kónya, I. Kiricsi, Carbon 43 (2005) 994–1000.
[17] T. Kanyó, J. Zhu, K. Niesz, D. Mehn, I. Kiricsi, Carbon 42 (2004) 2001–2008.
[18] H.S. Kim, B.H. Park, J.S. Yoon, H.-J. Jin, Eur. Polym. J. 43 (2007) 1729–1735.
[19] C. Lia, T.W. Chou, Appl. Phys. Lett. 90 (2007) 174108.
[20] S.H. Yao, Z.M. Dang, M.J. Jiang, H.P. Xu, Appl. Phys. Lett. 91 (2007) 212901.
[21] J. Li, P.C. Ma, W.S. Chow, C.K. To, B.J. Tang, J.K. Kim, Adv. Funct. Mater. 17 (2007) 3207–3215.
[22] R. Jung, H.S. Kim, Y. Kim, S.M. Kwon, H.S. Lee, H.-J. Jin, J. Polym. Sci. Polym. Phys. 46 (2008) 1235–1242.
[23] C.A. Poland, R. Duffin, I. Kinloch, A. Maynard, W.A.H. Wallace, A. Seaton, V. Stone, S. Brown, W. MacNee, K. Donaldson, Nat. Nanotechnol. 3 (2008) 423–428.
[24] J.C. Charlier, Acc. Chem. Res. 35 (2002) 1063–1069.
[25] R. Gao, Z.L. Wang, S. Fan, J. Phys. Chem. B 104 (2000) 1227–1234.
[26] H. Yu, Y. Jin, F. Peng, H. Wang, J. Yang, J. Phys. Chem. C 11 (2008) 6758–6763.
[27] R. Andrews, D. Jacques, D. Qian, E.C. Dickey, Carbon 39 (2001) 1681–1687.
[28] C.L. Zhang, H.S. Shen, J. Phys.: Condens. Matter. 19 (2007) 386212.
[29] D. Bom, R. Andrews, D. Jacques, J. Anthony, B. Chen, M.S. Meier, J.P. Selegue, Nano Lett. 2 (2002) 615–619.
[30] S. Porro, S. Musso, M. Vinante, L. Vanzetti, M. Anderle, F. Trotta, A. Tagliaferro, Physica E 37 (2007) 58–61.
[31] H.S. Kim, W.I. Park, M. Kang, H.-J. Jin, J. Phys. Chem. Solids 69 (2008) 1209–1212.
[32] D.M. Ren, Z. Guo, F. Du, Z.F. Liu, Z.C. Zhou, X.Y. Shi, Y.-S. Chen, J.-Y. Zheng, Int. J. Mol. Sci. 9 (2008) 45–55.
[33] H.S. Lee, C.H. Yun, H.M. Kim, C.J. Lee, J. Phys. Chem. C 111 (2007) 18882–18887.